J Fusion Energ (2015) 34:1175–1180
DOI 10.1007/s10894-015-9941-4

ORIGINAL RESEARCH

Influence of the Collisions on the Dusty Plasma Sheath in the Presence of an Oblique Magnetic Field

F. Nafari[1] · M. Ghoranneviss[1] · K. Yasserian[2]

Published online: 17 May 2015

Abstract The dust dynamics in a magnetized collisional plasma-sheath are numerically studied by using the fluid model. Isothermal electrons, cold fluid ions, cold fluid dust grains and immobile neutral particles are taken into account in the sheath. As dust can be created by detaching small pieces of the wall limiting plasma, naturally, these grains can have different sizes. Therefore, the influence of dust size on the sheath characteristics is considered. Assuming the dust–neutral collision cross section has a power law dependency on the dust velocity. The comparison of the effect of the dust radius in both specific collisional models shows that in the constant cross section model, dust size plays a more role with respect to the constant collision frequency. The effect of the dust size on dust velocity is investigated for different values of the power factor. It shows that dust velocity when reaching near the wall in constant cross section model is much less than constant mobility model, and the velocity of the smaller dust is lower on the wall. If dust density is very small, the kind of collisional model has no significant influence on the electric potential. But by increasing dust density, a little fall in the local electric potential and a little rise in the sheath thickness are seen in constant cross section model.

Keywords Plasma-sheath · Dust grains · Collisional force · Constant cross section model · Constant collisional mobility model

✉ F. Nafari
f_nafari@yahoo.com

[1] Plasma Physics Research Center, Science and Research Branch, Islamic Azad University, Tehran, Iran

[2] Department of Physics, Faculty of Sciences, Karaj Branch, Islamic Azad University, Karaj, Iran

Introduction

In the steady state condition, a surface located inside the plasma attains a negative potential with respect to the plasma core. This potential cannot spill over to the plasma due to the Debye shielding. Therefore, the positive ions accelerate toward, while the electrons repel from the wall in which lead to formation of layer of space charge that is called plasma sheath [1, 2].

The dust particles can be introduced artificially in a plasma-sheath or may appear as the impurity contaminants, which are added by production tools and processes. The presence of dense clouds of dust particles near the wall essentially changes the plasma-sheath behavior and a new dissipative sheath structure can be formed [3].

In addition, depending on the ambient plasma conditions, dust particles can carry both negative as well as positive charge [4].

Some earlier studies have considered the effects of the electrostatic, gravitational, external magnetic field and collision force on dust characteristics [5–10].

Liu et al. [8] studied the characteristics of dust plasma-sheath in an oblique magnetic field using the fluid method in which the authors showed that under the action of magnetic force, the dust grains make helical movements and some fluctuations in distribution of dust density emerge.

In Ref. [10], dusty plasma sheath is investigated by considering the constant collisional mobility in various dust sizes. Their results showed that the dust having smaller radius carries more obvious magnetic field effects on it. In a same external magnetic field, there are less fluctuations and the dust gyro radius is bigger for the dust with bigger radius (i.e., the collision effects increase by increasing the radius of dust).

In this paper, the main goal is to investigate the effect of the dust sizes on the characteristics of the collisional magnetized dusty plasma sheath where the dust–neutral collision cross section has the power law dependency on dust flow velocity. Based on some earlier studies [8–10], the fluid model is used for a dusty plasma sheath. We simultaneously consider the effects of the electromagnetic, gravitation, and collision forces on the dust characteristic, by taking into consideration the effect of the kind of collision model in the presence of dusts with different sizes. The present sheath consists of the electrons in equilibrium thermal, cold fluid ions in collisionless regime, cold fluid charged dust grains and immobile neutral particles.

This work is organized as follow. In "Basic Equations and Assumptions" section, the governing equations are presented, and the set of dimensionless quantities is introduced. In "Numerical Results" section , the equations are numerically solved. The main results are summarized in "Conclusions" section.

Basic Equations and Assumptions

We consider a magnetized dusty plasma sheath in contact with a planar wall, which has one dimension coordinate space and three dimensions in speed space. The constant external magnetic field is embedded in the x–z plane. The x-direction is taken as the direction of gravitational force and the direction of variations of the physical parameter and the depth direction from the plasma edge to the wall (see Fig. 1). At the edge of the sheath $x = 0$, the electrostatic potential is taken to be zero, and the ion, electron and dust densities n_{i0}, n_{e0}, n_{d0} satisfy the quasi-neutrality condition $e(\mathrm{n}_{i0} - \mathrm{n}_{e0}) + q_{d0}n_{d0} = 0$, where e, q_{d0} are the electron charge and dust charge at the sheath edge, respectively.

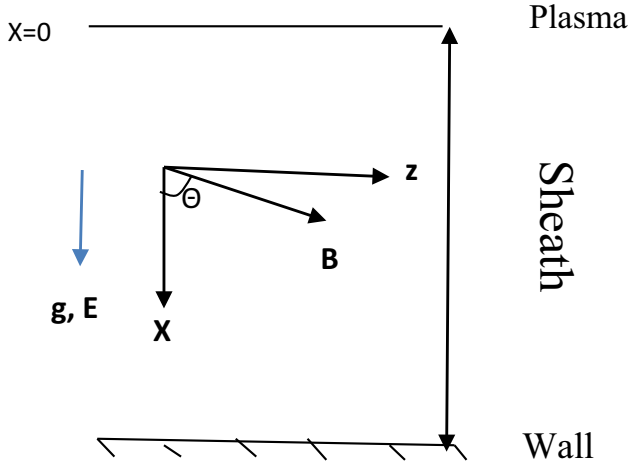

Fig. 1 The geometry of the sheath model

It is assumed that the sheath is consisting of isothermal electrons, cold fluid ions, cold fluid charged dust grains and immobile neutral particles.

Since the electrons are in the isothermal equilibrium therefore, they are distributed according to Boltzmann relation [11–15].

$$n_e = n_{e0}\exp\left(\frac{e\varphi}{kT_e}\right) \tag{1}$$

where φ is the electrostatic potential, T_e is the electron temperature and n_{e0} is the electron density at the sheath edge.

We assume $\lambda_d \approx \lambda_e$ and $\lambda_i \gg \lambda_e$ where λ_e, λ_i and λ_d are electron deby lengh, ion and the dust mean free path, respectively. This means that we are in a regime of ion-neutral collisionless and dust–neutral collisional. This regime has been considered elsewhere [16, 17].

The cold fluid ion equations are:

$$\frac{\partial(n_i v_i)}{\partial x} = 0 \tag{2}$$

$$v_i\frac{\partial(v_i)}{\partial x} = -\left(\frac{e}{m_i}\right)\frac{\partial\varphi}{\partial x} \tag{3}$$

where m_i, n_i and v_i are the mass, density and velocity of ion. We assume that magnetic field cannot affect ion density distribution directly [8–10]. This assumption is valid, because the mean effect of the magnetization of ions on their movement is zero. This is due to the fact that movement of dust grains is far slower than that of the ions, and so the ions are excessively magnetized.

Among the models developed to study the dusty plasma [18–20], we use the fluid model since the micron-sized dust grains, when dust density is not very small are collectively treated as fluid. For charged dust grains, the continuity and momentum equations are as follows:

$$\frac{\partial(n_d v_d)}{\partial x} = 0 \tag{4}$$

$$m_d v_{dx}\frac{\partial\vec{v}_d}{\partial x} = -q_d\frac{\partial\varphi}{\partial x}\hat{x} + q_d\vec{v}_d \times \vec{B}_0 + m_d g\hat{x} + \vec{F}_c \tag{5}$$

where n_d, m_d, v_d and q_d are the density, mass, velocity and charge of the dust, respectively. $\vec{F}_C$ is the neutral collisional force as follow:

$$\vec{F}_c = -m_d v_{dn}\vec{v}_d \tag{6}$$

where v_{dn} is the collision frequency between dust grains and neutrals which is generally given by the following relation:

$$v_{dn} = n_n\sigma v_d \tag{7}$$

Here n_n is the neutral gas density, σ is momentum transferring cross section between dust grains and neutrals and v_d is dust velocity.

In general case, the cross section has the power law dependence on dust velocity as follow [21–24]:

$$\sigma = \sigma_s \left(\frac{v_d}{c_{ds}}\right)^p \tag{8}$$

where p (i.e., pawor factor) is the dimensional parameter, depending on type and pressure of neutral gas, that can change from -1 to 0, c_{ds} is the dust acoustic velocity and σ_s is the cross section measured at dust acoustic velocity.

There are usually two special aspects to cross section σ: constat cross section model corresponding to $p = 0$ and constat mobility model corresponding to $p = -1$. In the first model, the collision frequency depends linearly on dust velocity while, in the second model, the cross section depends inversely on dust velocity, and therefore the collision frequency is independent of velocity. Here we consider the dust as spherical particle with constant mass, $m_d = \frac{4}{3}\pi R^3 \rho$ where R is the dust radius and ρ is the mass density of dust grains.

The model is completed with the poisson equation.

$$\frac{\partial^2 \varphi}{\partial x^2} = -[e(n_i - n_e) + q_d n_d] \tag{9}$$

To solve the governing equations numerically, some dimensionless quantities are introduced as

$$M_i = \frac{v_{ix0}}{c_{is}}, \eta = \frac{-e\varphi}{T_e}, N_e = \frac{n_e}{n_{e0}}, N_i = \frac{n_i}{n_{i0}}, N_d = \frac{n_d}{n_{d0}}, \xi = \frac{x}{\lambda_e}$$

where M_i is the ion mach number, v_{ix0} is the ion velocity at the sheath edge, $c_{is} = (T_e/m_i)^{0.5}$ is the ion sound speed, n_{e0}, n_{i0} and n_{d0} are the electron, ion and dust density distribution at the sheath edge. As we are going to compare the dust dynamics with different radiuses, we normalized the dust velocity with the dust sound speed that has specific radius 'a'. We hinted the dust characteristics of this reference radius with 'a' as superscript, so $c_{ds}^{(a)} = \left(T_e \Big/ m_d^{(a)}\right)^{0.5}$. We assume that dust mass density is constant, and the dust sound speed that has radius R is; $c_{ds} = c_{ds}^{(a)}(a/R)^{1.5}$. Thus, the dimensionless dust velocity is $u_d = v_d \Big/ c_{ds}^{(a)}$.

By substituting these dimensionless quantities into the governing Eqs. (1)–(9), we obtain.

$$n_e = \exp(-\eta) \tag{10}$$

$$N_i = \left(\frac{2\eta}{M_i^2 + 1}\right)^{-\frac{1}{2}} \tag{11}$$

$$N_d = \frac{M_d}{u_{dx}} \left(\frac{a}{R}\right)^{\frac{3}{2}} \tag{12}$$

$$u_{dx}\frac{\partial u_{dx}}{\partial \xi} = \left(\frac{a}{R}\right)^3 \left(z_d \frac{\partial \eta}{\partial \xi} + \gamma z_d \sin\theta u_{dy}\right) + \mu - \left(\frac{a}{R}\right)^{4+3p} \alpha u_d^{p+1} u_{dx} \tag{13}$$

$$u_{dx}\frac{\partial u_{dy}}{\partial \xi} = \left(\frac{a}{R}\right)^3 \gamma z_d (\cos\theta u_{dz} - \sin\theta u_{dx}) - \left(\frac{a}{R}\right)^{4+3p} \alpha u_d^{p+1} u_{dy} \tag{14}$$

$$u_{dx}\frac{\partial u_{dz}}{\partial \xi} = -\left(\frac{a}{R}\right)^3 \gamma z_d \cos\theta u_{dy} - \left(\frac{a}{R}\right)^{4+3p} \alpha u_d^{p+1} u_{dz} \tag{15}$$

$$\frac{\mathrm{d}^2\eta}{\mathrm{d}\xi^2} = z_d \delta_d N_d + \delta_i N_i - N_e \tag{16}$$

where $M_d = \frac{v_{dx0}}{c_{ds}}, \delta_i = \frac{n_{i0}}{n_{e0}}, \delta_d = \frac{n_{d0}}{n_{e0}}, z_d = \frac{q_d}{e}, \gamma = \left(\frac{\varepsilon_0}{n_{e0} m_d^{(a)}}\right)^{0.5} B_0, \mu = g\lambda_e \frac{m_d^{(a)}}{T_e}$ and $\alpha = \lambda_e n_n \sigma_s^{(a)}$ where $\sigma_s^{(a)}$ is the collision cross section measured at dust sound speed for dust grain having radius 'a'.

Numerical Results

In this section, we attempt to solve the basic equations via the Runge–Kutta method. In the following numerical results we adopt the parameters as;

$$z_d = -1000, a = 4\,\mu\mathrm{m}, \rho_m = 2\frac{gr}{\mathrm{cm}^3},$$

$$T_e = 2ev, \frac{\partial \eta}{\partial \xi}|_{\xi=0} = 0.01, \delta_i = 1.01, \delta_d = 10^{-5}, M_d = 1.1$$

The parameters are considered the same as used by Liu et al. and Masoudi et al. [8–10]. Therefore, we can compare our results with their results.

It is assumed that dust grains enter the sheath perpendicularly to the sheath boundary; $u_{dy}|_{\xi=0} = u_{dz}|_{\xi=0} = 0$.

In Fig. 2 we have presented the dust velocity profile versus dust radius in the constant collisional mobility model; $p = -1(\alpha = 7, \gamma = 0.3, \theta = 40^\circ)$ which is in agreement with the Ref. [10].

The figure shows that the magnetic field corresponding to $\gamma = 0.3, \theta = 40^\circ$ is strong enough to make fluctuations in dust velocity that has radius 4 μm in a magnetic collisional plasma-sheath. However, for larger values of radius, the fluctuations decrease.

In Fig. 3, the same plot is presented in the constant cross section model; $p = 0$.

It can be seen that in constant cross section model there are no fluctuations in dust velocity for three different dust

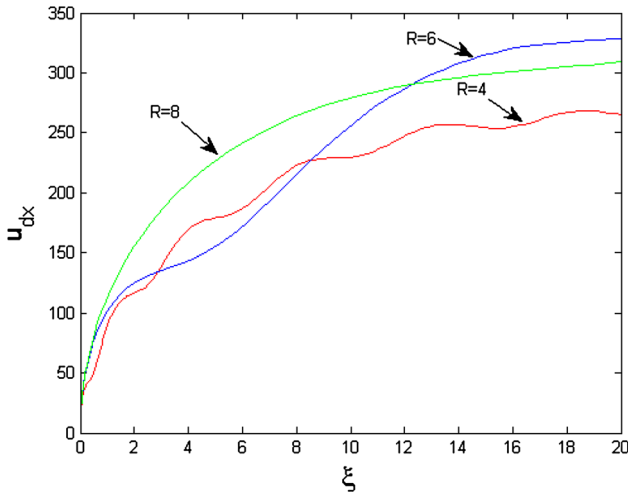

Fig. 2 The profile of dust velocity for three different dust radius in the constant collisional mobility model ($\alpha = 7, \gamma = 0.3, \theta = 40°$)

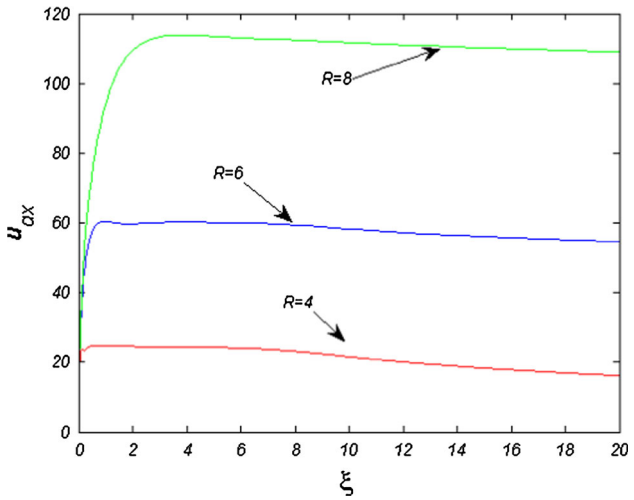

Fig. 3 The profile of dust velocity for three different radiuses in constant collision cross section ($\alpha = 7, \gamma = 0.3, \theta = 40°$)

radiuses since the magnetic field is not strong enough to make fluctuations in dust velocity in depth direction.

By comparison of Fig. 2 with Fig. 3, one can conclude that in constant cross section model in addition to disappearing fluctuations, dust velocity becomes slower. As the collision force can decrease the fluctuations in dust velocity in depth direction. So in this model, dust grains experience more collisional force through the sheath and the influence of the magnetic field on dusts diminishes. The derivation of the collision force equation between dust grains and neutral particles, given in the "Appendix", shows that in constant cross section model, the collision force is proportional to dust velocity square, and in constant mobility model the collision force depends directly on dust velocity. i.e., in a same dust velocity, the friction force is more in constant

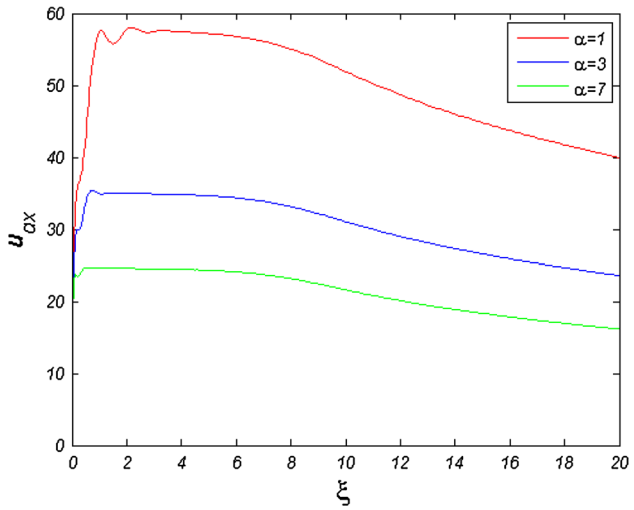

Fig. 4 The profile of dust velocity for three different collision amplitude in constant cross section model ($\gamma = 0.3, \theta = 40°$)

cross section model compared with constant mobility model. Hereby, the above-mentioned results can be confirmed.

Now, we focus on the influence of collision and magnetic force on the profile of dust velocity in constant cross section model. As shown in Fig. 2, in a same external magnetic field, there are more fluctuations in the dust with smaller radius. Therefore, we consider $R = 4$.

In Fig. 4 the dust velocity profile is presented as a function of collisional amplitude in constant cross section model.

The figure shows that for lower collisional amplitude, a fluctuations in dust velocity near the sheath edge appear. But, by increasing distance from the sheath edge, the fluctuations vanish quite, i.e., by increasing distance from the sheath edge, the collision force eliminates the fluctuations. In addition, the increasing of the collision amplitude causes the dust velocity to reduce more.

In Fig. 5 we have presented the dust velocity profile in collisional case and collisionless case with R = 4.

As the figure shows, the difference in dust velocity between a constant collisional mobility model and collisionless case is very little in the near sheath edge. While, this difference will be more by increasing the distance from the sheath edge. But, the difference in dust velocity between a constant collisional cross section model and collisionless case is very more. Therefore, the effect of the collision force is more in constant collisional cross section model.

To concentrate on the effect of a power factor on the sheath region, we have plotted the dust velocity at the end of the sheath ($\xi = 20$) as a function of p for three different dust radiuses.

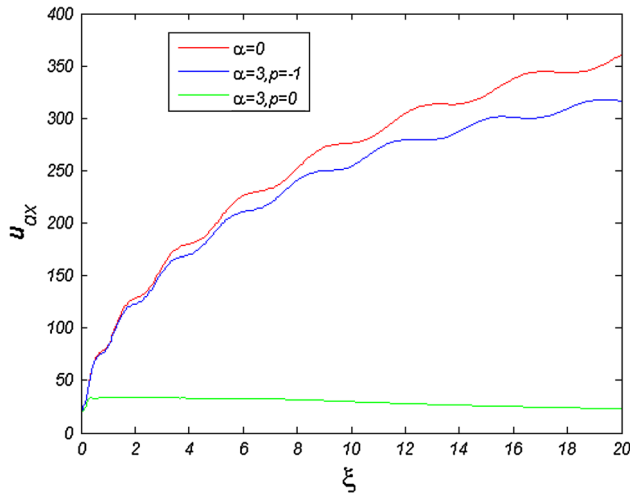

Fig. 5 The profile of dust velocity in collision case and collisionless case with R = 4 ($\gamma = 0.3, \theta = 40^\circ$)

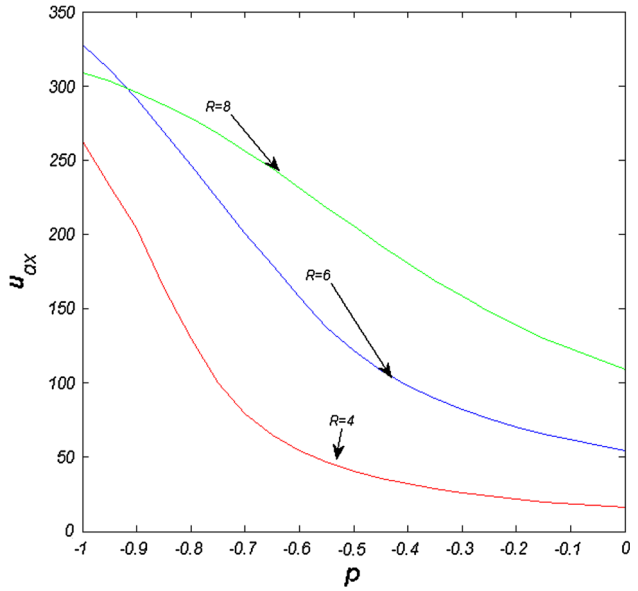

Fig. 6 The dust velocity at the end of the sheath versus power factor for three different dust radiuses ($\alpha = 7, \gamma = 0.3, \theta = 40^\circ$)

According to Fig. 6, by increasing the power factor the dust velocity decreases, and the dust velocity that has smaller radius will decrease more. In constant cross section model, the dust velocity when reaching near the wall is much less than constant collisional mobility model, and the velocity of the smaller dust is lower on the wall.

Figure 7 shows the electrostatic potential in depth direction for two collision models.

If dust density is very small, the kind of collisional model has no significant influence on the electric potential, and the electrostatic potential is the same for two models. But by increasing ten times for dust density, we can see

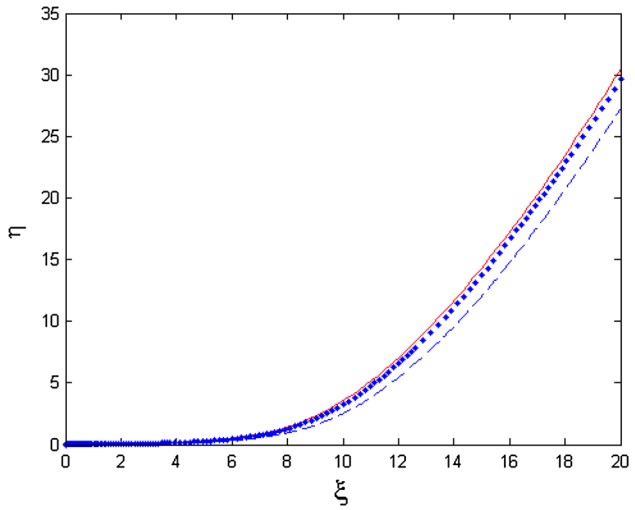

Fig. 7 The profile of the electric potential for $\delta_d = 10^{-5}$, $p = 0$, $p = -1$ (*solid line*); $\delta_d = 10^{-4}$, $p = 0$ (*dashed line*); $\delta_d = 10^{-4}$, $p = -1$ (*square line*) ($\alpha = 7, \gamma = 0.3, \theta = 40^\circ$)

that there is a little drop in the local electric potential and a bit rise in the sheath thickness (the distance between the sheath edge and the wall with constant electric potential) in constant collisional cross section model comparing with constant mobility model. In constant cross section model compared with constant collisional mobility model, the effect of the friction force brings more decrease in the dust velocity. Because of the inverse relation between the velocity in depth direction and the dust density, the more decrease of the dust velocity would lead to more increase of the dust density N_d. From the Poisson equation, this would cause more decrease of the electrostatic potential η.

Conclusions

Magnetized collisional dusty plasma sheath is studied numerically by using the fluid model. The electromagnetic, gravitational and dust–neutral collisional force affect the cold fluid dust with different sizes. To generalize the collisional plasma sheath problem, it is assumed that the cross section for collisions between dust and neutral has a power law dependency on the dust velocity. We found that dust size play more role in constant collision cross section model as the effects of collisions are more apparent in this model and fluctuations diminish. The dust velocity near the wall was carefully scanned for whole range of the power factor. It is observed that by increasing the power factor, the dust velocity decreases. This scanning reveals that in constant cross section model, near the wall, dust velocity is much slower with respect to the constant collisional mobility model. Also, the velocity of the smaller dust is slower near the wall. Our results show that in low concentration of

dust, the electric potential is independent of the power factor while in high concentration of dust, the local electric potential is a little decreased, and the sheath thickness is a bit increased in constant collisional cross section model.

Appendix: Derivation of the Dust–Neutral Collision Force

The dust−neutral collision force is : $\vec{F}_c = -m_d \nu_{dn} \vec{v}_d$ (17)

The collision frequency is: $\nu_{dn} = n_n \sigma v_d$ (18)

The cross section is: $\sigma = \sigma_s \left(\frac{v_d}{c_{ds}} \right)^p$ (19)

By substituting the value of σ from Eq. 19 into Eq. 18, then substituting the new value of ν_{dn} into Eq. 19. We obtain the new value of the dust–neutral collision force as follow:

$$\vec{F}_c = -m_d n_n \sigma_s \left(\frac{v_d}{c_{ds}} \right)^p v_d \vec{v}_d \Rightarrow \vec{F}_c = \begin{cases} -m_d n_n \sigma_s v_d \vec{v}_d & if \quad p = 0 \ (cross\ section\ model) \\ -m_d n_n \sigma_s c_{ds} \vec{v}_d & if \quad p = -1 \ (constant\ mobility\ model) \end{cases} \quad (20)$$

Equation 20 shows that in constant cross section model, the collision force is proportional to dust velocity square, and in constant mobility model the collision force depends directly on dust velocity.

References

1. K. Yasserian, M. Aslaninejad, M. Ghoranneviss, F.M. Aghamir, J. Phys. D Appl. Phys. **41**, 105215 (2008)
2. K. Yasserian, M. Aslaninejad, M. Borghei, M. Eshghabadi, Theor. Appl. Phys. **4**(2), 26–29 (2010)
3. H. Mehdipour, I. Denysenko, K. Ostrikov, Phys. Plasmas **17**, 123708 (2010)
4. B.P. Pandey, A.A. Samarian, S.V. Vladimirov, J. Plasma Fusion Res. Ser. **8**, 385–388 (2009)
5. S.W. Kang, K.W. Min, E.S. Lee, J. Seon, J. Surf. Coat. Technol. **7**, 171 (2003)
6. K.U. Riemann, Phys. Plasmas **1**, 552 (1994)
7. G.C. Das, P. Kalita, J. Phys. D **4**, 702 (2004)
8. J.Y. Liu, Q. Zhang, X. Zou, Z.X. Wang, Y. Liu, X.G. Wang, Y. Gong, Vacuum **73**, 68 (2004)
9. S.F. Masoudi, G.R. Jafari, H.A. Shorakaee, Vacuum **83**, 1031 (2009)
10. S.F. Masoudi, P. Taherparvar, J. Fusion Energ. **29**, 240–243 (2010)
11. F. Valsaque, G. Manfredi, J. Nucl. Mater. **763**, 290–293 (2001)
12. P.C. Stangeby, Phys. Plasmas **2**, 702 (1995)
13. T.E. Sheridan, J. Goree, Phys. Fluids B **3**, 2796 (1991)
14. S.K. Baishya et al., Phys. Plasmas **6**, 3678 (1999)
15. S.K. Baishya, G.C. Das, Phys. Plasmas **10**, 3733 (2003)
16. P. Duan, J. Liu, Y. Gong, Y. Liu, X. Wang, Plasma Sci. Technol. **9**, 394 (2007)
17. X. Zou, Chin. Phys. Lett. **23**, 396 (2006)
18. Z.X. Wang, W. Wang, Y. Liu, X. Wang, Chin. Phys. Lett. **21**, 697 (2004)
19. J.X. Ma, M.Y. Yu, Phys. Plasmas **2**, 1343 (1995)
20. A. Barkan, R.L. Merlino, D. Angelo, Phys. Plasmas **2**, 35563 (1995)
21. S.F. Masoudi, S.M. Salehkoutahi, Eur. Phys. J. D **57**, 71–76 (2010)
22. S.F. Masoudi, Eur. Phys. J. D **64**, 369–373 (2011)
23. J.I. Yankun, Z. Xiu, L. Huiping, Plasma Sci. Technol. **13**(5), 519–522 (2011)
24. I. Driouch, Z. Chatei, Appl. Fluid Mech. **6**(4), 511–517 (2013)